

# Microstructure and Mechanical Properties of Tin-Bismuth Solder Reinforced by Aluminum Borate Whiskers

JUN WANG,<sup>1</sup> HONGMEI WEI,<sup>1</sup> PENG HE,<sup>1,3</sup> TIESONG LIN,<sup>1</sup>  
and FENGJIAO LU<sup>2</sup>

1.—State Key Laboratory of Advanced Welding and Joining, Harbin Institute of Technology, Harbin 150001, China. 2.—Shuangliang Eco-Energy Systems Co., Ltd., Jiangyin 214444, China. 3.—e-mail: hithepeng@hit.edu.cn

Tin-bismuth solder has emerged as a promising lead-free alternative to tin-lead solder, especially for low-temperature packaging applications. However, the intrinsic brittleness of tin-bismuth solder alloy, aggravated by the coarse bismuth-rich phase and the thick interfacial intermetallic layer, notably limits the mechanical performance of the bonded joints. In this work, the microstructure and mechanical performance of solder joints were improved by adding 3.2 vol.% aluminum borate whiskers to the tin-bismuth solder alloy. This whisker-reinforced composite solder was fabricated through a simple process. Typically, 25- $\mu\text{m}$  to 75- $\mu\text{m}$  tin-bismuth particles were mixed with a small amount of aluminum borate whiskers with diameter of 0.5  $\mu\text{m}$  to 1.5  $\mu\text{m}$  and length of 5  $\mu\text{m}$  to 15  $\mu\text{m}$ . The addition of whiskers restrained the formation of coarse brittle bismuth-rich phase and decreased the lamellar spacing from 0.84  $\mu\text{m}$  to 7.94  $\mu\text{m}$  to the range of 0.22  $\mu\text{m}$  to 1.80  $\mu\text{m}$ . Moreover, the growth rate of the interfacial intermetallic layer during the remelting treatment decreased as well. The joint shear strength increased from 19.4 MPa to 24.7 MPa, and only declined by 4.9% (average, -5.9% to 15.8%) after the tenth remelting, while the shear strength of the joint without whiskers declined by 31.5% (average, 10.1–44.1%). The solder alloy was reinforced because of their high strength and high modulus and also the refinement effect on the solder alloy microstructure.

**Key words:** Tin-bismuth alloy, aluminum borate whiskers, composite solder, shear strength

## INTRODUCTION

Tin-bismuth (Sn-Bi) solder is one of the most promising lead-free alternatives for use in packaging applications below 200°C due to its low eutectic temperature.<sup>1–3</sup> Therefore, thermal damage can largely be avoided during the assembly process, leading to improved microelectronic packaging reliability.<sup>1</sup> However, application of Sn-Bi solder is limited by unsatisfactory joint strength due to the brittle nature of the coarse Bi-rich phase and thick interfacial intermetallic layer, especially if the joint is annealed or applied in high-temperature

conditions.<sup>2,3</sup> It is thus essential to modify the microstructure and improve the mechanical properties of Sn-Bi solder to achieve satisfactory reliability for further applications.

Addition of reinforcement materials, such as carbon nanotubes, metal oxides, metallic nanoparticles, etc., is an effective way to modify the microstructure and enhance the mechanical properties of solder alloys.<sup>4–7</sup> Among such materials, whiskers perform well as reinforcement materials to improve the mechanical properties of various metallic and ceramic composites.<sup>8–10</sup> The hardness and bending strength of a copper matrix were both improved by adding a small amount of whiskers.<sup>11,12</sup> The strength of aluminum alloy or titanium alloy was also reinforced by addition or *in situ*

(Received September 7, 2013; accepted June 10, 2015; published online July 3, 2015)

growth of whiskers.<sup>13,14</sup> Such whiskers, which have diameters ranging from 0.2  $\mu\text{m}$  to 2  $\mu\text{m}$  and lengths less than 100  $\mu\text{m}$ , are easily dispersed in composites.<sup>15,16</sup> Thus, whiskers are a suitable material for reinforcement of tiny joints in microelectronic packaging applications.<sup>17</sup> It has been reported that SbSn and  $\text{Cu}_6\text{Sn}_5$  whiskers formed in tin-based solder joints effectively improved the creep resistance or work-hardening rate.<sup>18,19</sup> A Pb-free solder composite containing NiTi fibers exhibited superplastic characteristics during tensile testing.<sup>20</sup> Joints reinforced by TiB whiskers also showed high shear strength.<sup>21</sup> Carbon fibers have also been used to improve the mechanical performance and thermal conductivity of joints.<sup>22</sup> However, although many kinds of ceramic whiskers, such as aluminum borate whiskers and silicon carbide whiskers,<sup>13,23</sup> have been applied to reinforce various metals and alloys, they have not been reported in composite solders. Silicon carbide particles have been applied to enhance the mechanical performance of lead-free solder, but whiskers have a more favorable influence on elastic-plastic properties and stiffness.<sup>24–26</sup> Silicon carbide whiskers have been found to notably enhance various aspects of mechanical performance such as compressive strength,<sup>27</sup> superplasticity,<sup>28</sup> and fracture toughness.<sup>29</sup> However, aluminum borate whiskers show higher tensile strength and Young's modulus compared with silicon carbide whiskers,<sup>30,31</sup> and metallic composites with aluminum borate whisker fillers exhibit even better mechanical performance.<sup>32</sup> Additionally, the price of aluminum borate whiskers is far below that of silicon carbide whiskers, so there is great potential for application of aluminum borate whiskers in large-scale industrial manufacturing processes. The purpose of this work is to investigate the effect of aluminum borate whiskers on the microstructure and strength of tin-bismuth alloy-based composites and soldered joints.

## EXPERIMENTAL PROCEDURES

The diameters of the regular spherical Sn-58Bi particles used in this experiment ranged from 25  $\mu\text{m}$  to 75  $\mu\text{m}$ , and the morphology of the particles is illustrated in Fig. 1a. Figure 1b correspondingly shows the morphology of the aluminum borate ( $\text{Al}_{18}\text{B}_4\text{O}_{33}$ ) whiskers. The whiskers were synthesized by high-temperature reaction of aluminum hydroxide and boric acid.<sup>33</sup> The whiskers grew into clavate single crystals with diameter of 0.5  $\mu\text{m}$  to 1.5  $\mu\text{m}$ , length of 5  $\mu\text{m}$  to 15  $\mu\text{m}$ , and length-to-diameter ratio of 5 to 30. The density of the whiskers was  $2.925 \pm 0.025 \text{ g/cm}^3$ .

The composite solder paste was prepared as follows:  $3.20 \pm 0.03 \text{ vol.}\%$   $\text{Al}_{18}\text{B}_4\text{O}_{33}$  whiskers were weighed and mixed with rosin flux (type Flux55) in an alumina crucible. Then, Sn-58Bi particles were gradually added into the mixture and stirred at 120 rpm until the whiskers were well distributed in the paste. The prepared composite solder paste was heated and remelted at 180°C on an oxygen-free copper plate for 180 s. A certain volume of paste was also heated at 180°C on an alumina ceramic plate for 90 s to fabricate solder balls. The molten solder

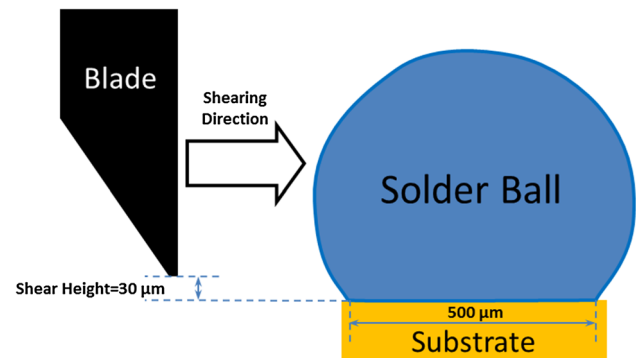


Fig. 2. Schematic of solder ball shear testing method.

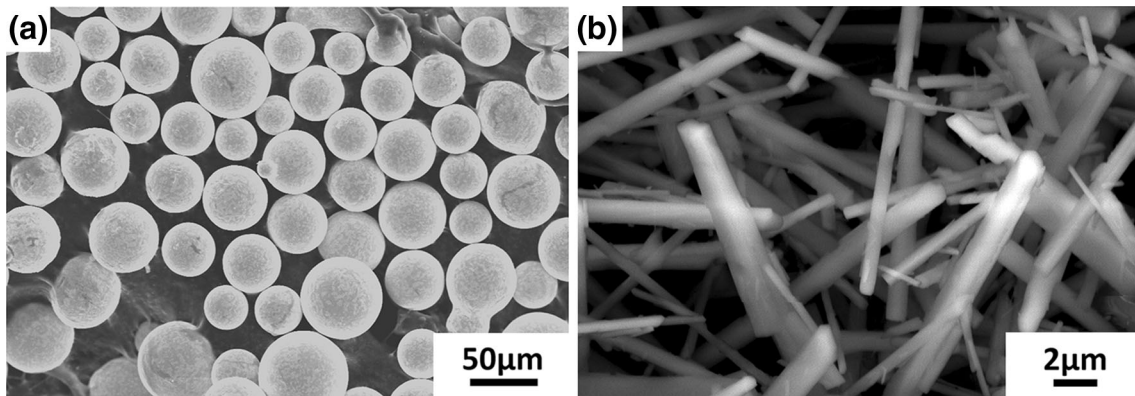


Fig. 1. (a) Original Sn-58Bi alloy particles and (b)  $\text{Al}_{18}\text{B}_4\text{O}_{33}$  whiskers.

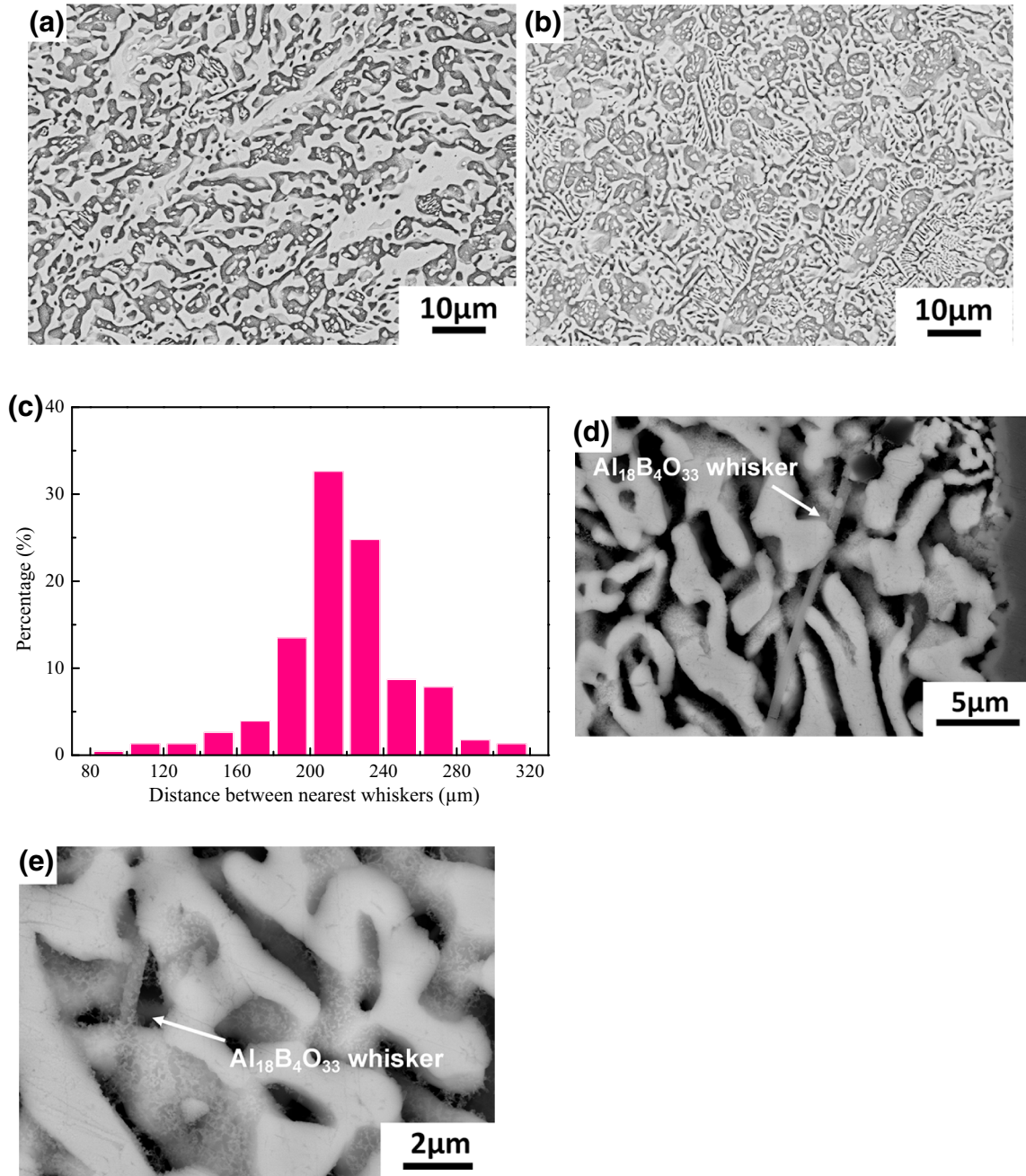


Fig. 3. Microstructure of (a) Sn-58Bi and (b) Sn-58Bi-3.2 vol.% $\text{Al}_{18}\text{B}_4\text{O}_{33}$ . (c) Distance between neighboring whiskers. (d, e) Whisker in Sn-58Bi-3.2 vol.% $\text{Al}_{18}\text{B}_4\text{O}_{33}$  composite solder.

transformed into spherical shape due to its non-wetting characteristic on alumina ceramic, and finally solidified as solder balls with diameter of  $600 \pm 20 \mu\text{m}$ . The solder balls were applied to ball grid array (BGA) joints bonding onto copper pads with diameter of  $500 \mu\text{m}$ . Solder balls were fixed on the pad with flux and remelted at the same temperature for one, three, five, eight, and ten times, respectively. To prepare samples for observation of intermetallic grains, redundant solder was cut with an electric discharge machine followed by treatment

with mixed solution of ethanol and nitric acid. The microstructure of the composite solder was analyzed by scanning electron microscopy (SEM, SU8020; Hitachi High-Technologies). The location coordinates of the whiskers were recorded using the accessory tools of the SEM, and the distance between neighboring whiskers was calculated from the location coordinates. The thickness and grain size of the intermetallic layer were analyzed using image analysis software (Nano Measurer 1.2). Shear strength was tested by the solder ball shear

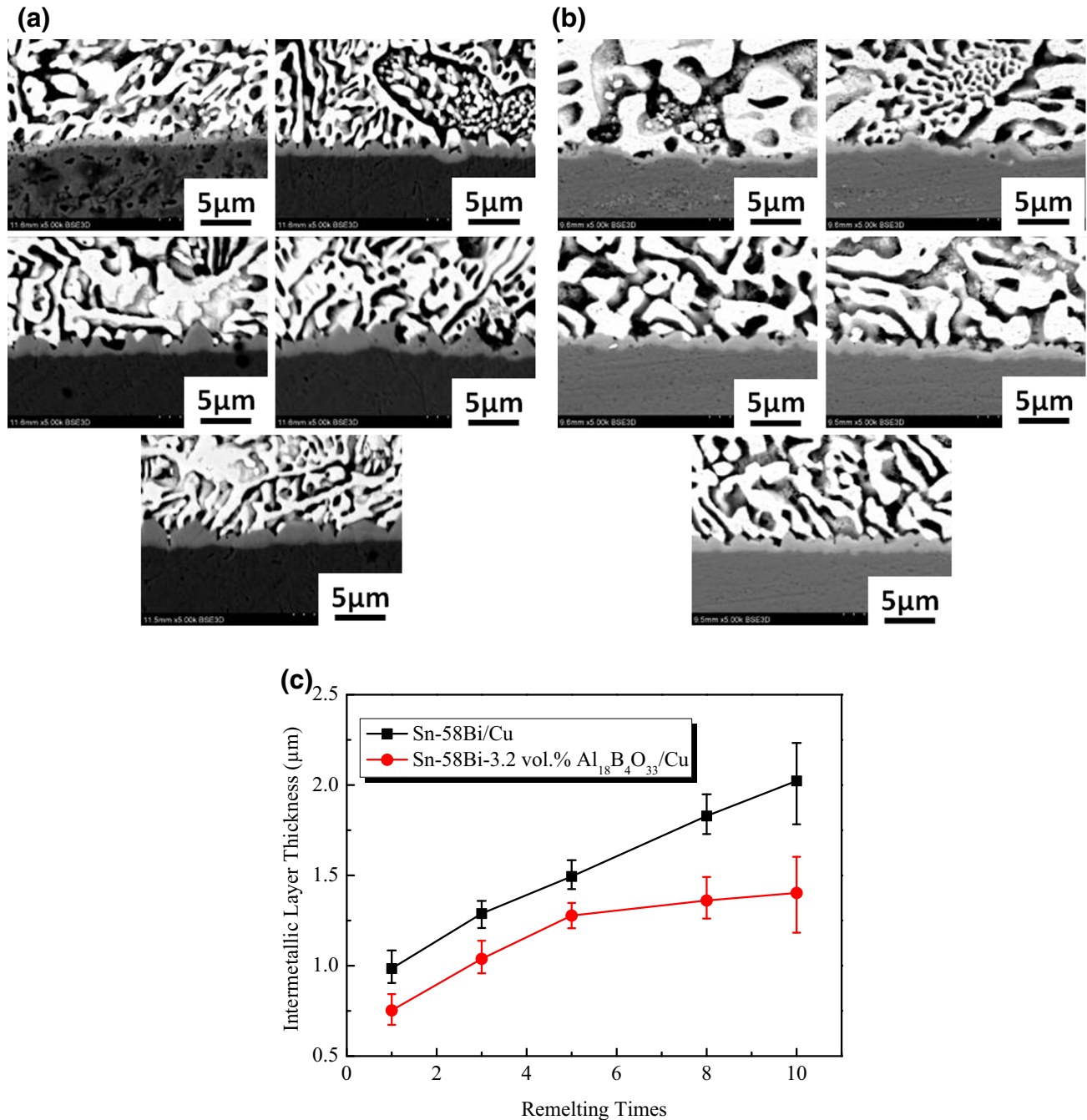


Fig. 4. Sections of intermetallic layer along (a) Sn-58Bi/Cu interface and (b) Sn-58Bi-3.2 vol.%Al<sub>18</sub>B<sub>4</sub>O<sub>33</sub>/Cu interface after different remelting times (from above: remelted for one, three, five, eight, and ten times) and (c) thickness of intermetallic layer along Sn-58Bi/Cu interface and Sn-58Bi-3.2 vol.%Al<sub>18</sub>B<sub>4</sub>O<sub>33</sub>/Cu interface after different remelting times.

testing method using a bond testing station (DAGE 4000; Nordson). As shown in Fig. 2, the shear blade moved along the shearing direction and deformed the solder ball bonded onto the substrate at a shear rate of 60 μm/s with shear height of 30 μm. The maximal shear force was recorded after each test, and 25 solder ball specimens were tested for each condition.

## RESULTS AND DISCUSSION

### Microstructure Evolution of Solder Alloy After Remelting

The microstructure of Sn-58Bi solder and Sn-58Bi-3.2 vol.%Al<sub>18</sub>B<sub>4</sub>O<sub>33</sub> composite solder after remelting is shown in Fig. 3. The microstructure of Sn-58Bi alloy solder was composed of white Bi-rich

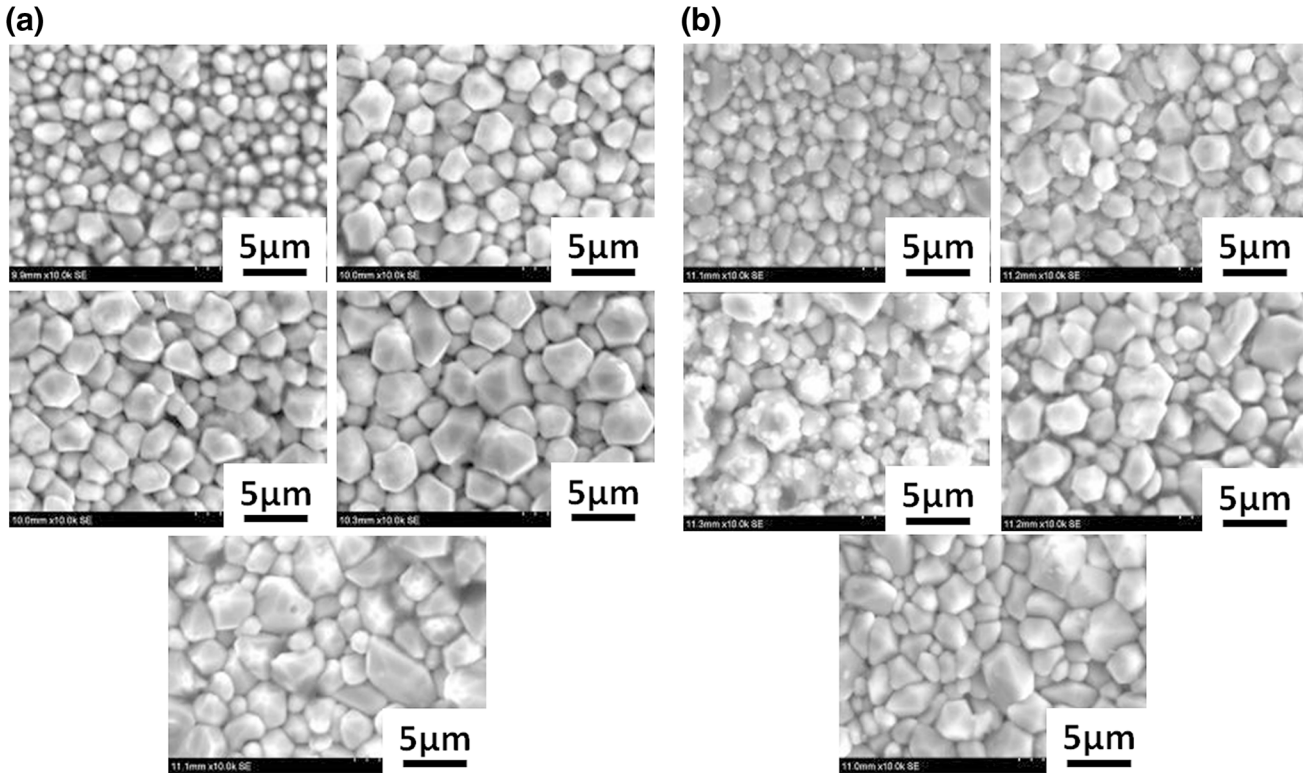


Fig. 5. Morphology of intermetallic layer along (a) Sn-58Bi/Cu interface and (b) Sn-58Bi-3.2 vol.%  $\text{Al}_{18}\text{B}_4\text{O}_{33}$ /Cu interface after different remelting times (from upper: remelted for one, three, five, eight, and ten times).

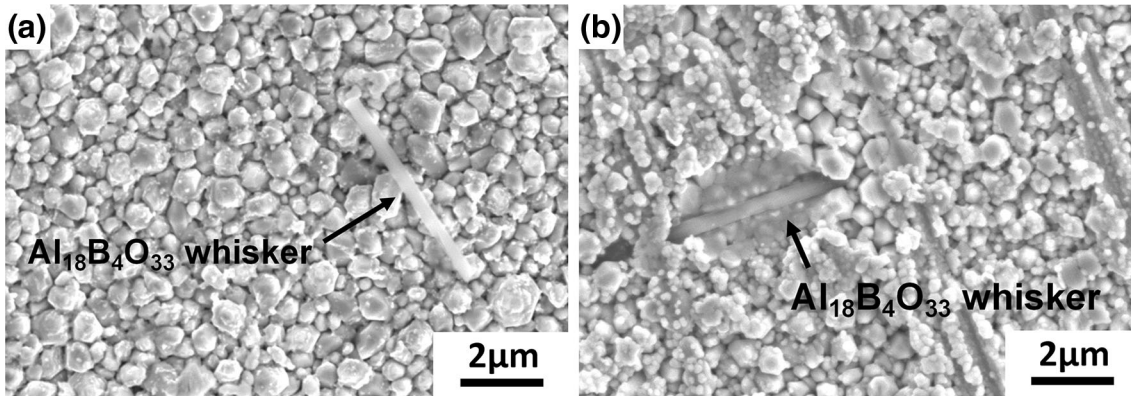


Fig. 6. Whiskers distributed (a) around the intermetallic layer and (b) in the intermetallic layer.

phase and dark Sn-rich phase, with the majority of the Bi-rich phase appearing as continuous network-like coarse structures with a few well-distributed Bi-rich phases observed in certain eutectic structures (Fig. 3a). By contrast, Bi-rich phases grew as fine lamellar eutectic dendrites after addition of  $\text{Al}_{18}\text{B}_4\text{O}_{33}$  whiskers (Fig. 3b). The lamellar spacing, i.e., the sum of the thicknesses of neighboring Sn-rich phase and Bi-rich phase layers, decreased from  $0.84 \mu\text{m}$  to  $7.94 \mu\text{m}$  to the range of  $0.22 \mu\text{m}$  to  $1.80 \mu\text{m}$ . In other words, the well-distributed whiskers induced microstructure refinement and homogenization of the Sn-58Bi alloy matrix. The

distance between neighboring whiskers is shown in Fig. 3c. The distance mainly ranged from  $190 \mu\text{m}$  to  $240 \mu\text{m}$ , showing a normal distribution with mean of  $217.4 \mu\text{m}$  and standard deviation of  $33.90 \mu\text{m}$ . This statistical result also indicates the homogeneity of the whisker distribution. Figure 3d and e illustrates the morphology of embedded  $\text{Al}_{18}\text{B}_4\text{O}_{33}$  whiskers that bonded well with the surrounding Sn-Bi alloy. The addition of whiskers effectively increased the nucleation rate and the number of heterogeneous nucleation sites during the cooling process. Furthermore, the well-distributed whiskers blocked crystal growth of Sn-Bi alloy and boosted

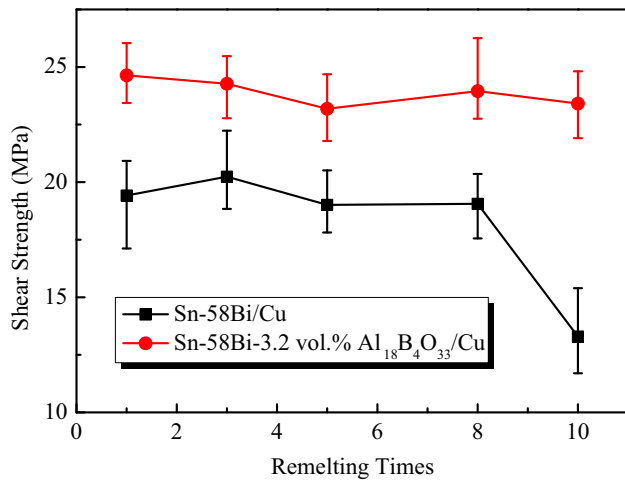


Fig. 7. Shear strength of bonded joint after different numbers of remelting treatments.

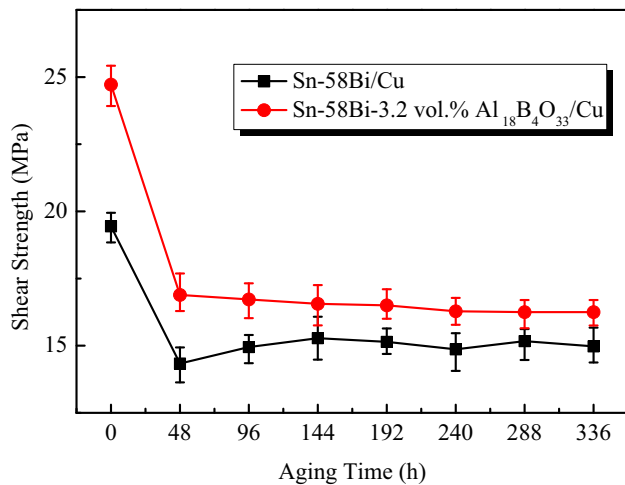


Fig. 8. Shear strength of bonded joints after aging treatment.

constitutional supercooling around phase boundaries, which diminished the lamellar spacing and improved the eutectic microstructure.<sup>34</sup>

### Microstructure Evolution of Intermetallic Layer After Remelting

Figure 4 illustrates the intermetallic layers along the interface of copper pad joints with and without Al<sub>18</sub>B<sub>4</sub>O<sub>33</sub> whiskers after remelting. The thickness of the layer along the Sn-58Bi/Cu interface increased almost linearly with the number of remelting times. By comparison, although the corresponding layer along the Sn-58Bi-3.2 vol.%Al<sub>18</sub>B<sub>4</sub>O<sub>33</sub>/Cu interface also became thicker after remelting, the increment of thickness was always quantitatively smaller, especially when remelted more than five times. This indicates a retardation effect on the growth rate of the intermetallic layer due to the addition of whiskers. This effect was more obvious than previously reported

with addition of other materials such as metallic nanoparticles.<sup>35</sup> Intermetallic grain sizes after different remelting times are shown in Fig. 5. It was observed that the grain size correlated positively with the remelting times despite the difference between the two solders, demonstrating Ostwald ripening of intermetallic grains that coarsened and merged with each other.<sup>36</sup> No obvious effect of whisker addition on the grain size of the intermetallic layer was observed, as the grain size distributions of both intermetallic layers were at the same level.

Figure 6 illustrates that Al<sub>18</sub>B<sub>4</sub>O<sub>33</sub> whiskers were inclined to adhere to the intermetallic layer to some extent and some whiskers even adhered to the copper pad and were surrounded by Cu<sub>6</sub>Sn<sub>5</sub> grains. The whiskers near the intermetallic layer could therefore block the Cu/Sn interdiffusion channel,<sup>37,38</sup> and thus the initial intermetallic layer could not grow as thick as the intermetallic layer without Al<sub>18</sub>B<sub>4</sub>O<sub>33</sub> whiskers due to the reduced diffusion rate.

### Shear Behavior After Remelting Treatment

The shear loading performance of BGA joints using Sn-58Bi solder with and without Al<sub>18</sub>B<sub>4</sub>O<sub>33</sub> whiskers after remelting is shown in Fig. 7, in which the error bars indicate the data scatter range of the measured shear strength values. It is seen that the shear strength of BGA joints with 3.2 vol.% Al<sub>18</sub>B<sub>4</sub>O<sub>33</sub> whiskers was relatively high compared with joints without whisker addition. The shear strength of the composite solder joints reached 24.7 MPa after one remelt, and only declined by 4.9% (average, -5.9% to 15.8%) to 23.4 MPa even after remelting ten times. The shear strength of the joints without whiskers declined remarkably by 31.5% (average, 10.1% to 44.1%) from 19.4 MPa to 13.3 MPa after the same remelting treatment. By contrast, aluminum alloy with 15 vol.% ceramic whiskers showed ca. 150% higher tensile strength, indicating the greater potential for shear strength improvement with a higher whisker concentration.<sup>8</sup> The shear load could be transmitted to the Al<sub>18</sub>B<sub>4</sub>O<sub>33</sub> whiskers with excellent strength and modulus. The shear strength of the BGA joints was effectively enhanced since most shear failure happened in the solder zone or at the solder/intermetallic interface. Besides, the addition of Al<sub>18</sub>B<sub>4</sub>O<sub>33</sub> whiskers played a positive role in the microstructure refinement of the solder, as the numerous phase boundaries and the whiskers themselves could hinder dislocation slip under the shear loading.

Figure 8 illustrates the relationship between the shear strength of BGA joints and the aging time. The error bars indicate the data scatter range of the measured shear strength values. The shear strength dramatically reduced after aging treatment under 90°C for 48 h, while it became almost stable after 96 h of aging treatment. Although the

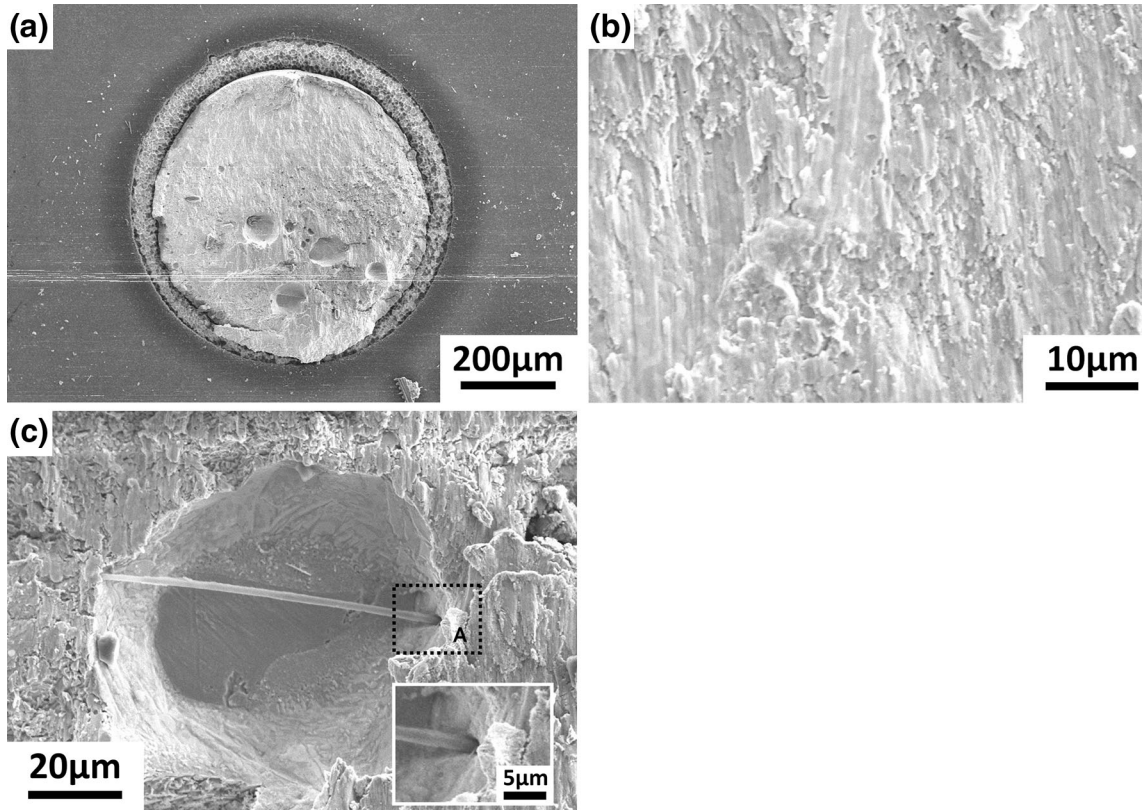


Fig. 9. (a–c) Fracture surface of BGA joint using Sn-58Bi-3.2 vol.% $\text{Al}_{18}\text{B}_4\text{O}_{33}$  composite solder remelted for one time after the shear test. The inset in (c) is a high-magnification image of zone A.

shear strength of the whisker-reinforced joints decreased by about one-third after 2 weeks of aging treatment, it was still 8.5% higher than that of Sn-Bi solder joints. For different samples at the same condition, the shear strength values showed a narrow distribution around the average. The maximum deviation of only 0.8 MPa shows the good coherence in the shear strength samples. The higher shear strength of the BGA joints with addition of 3.2 vol.% whiskers indicates that the whisker reinforcement improved the shear strength of the BGA joints even after aging treatment.

Figure 9 shows the fracture surface of a BGA joint using Sn-58Bi-3.2 vol.% $\text{Al}_{18}\text{B}_4\text{O}_{33}$  composite solder after the shear test. Fracture usually happened in the solder area under shear loading, as shown in Fig. 9a, and obvious plastic deformation could be found at the fracture surface. This illustrates that the whiskers enhanced the plastic deformation capability of the solder, and the stiffness of the BGA joints became smaller compared with BGA joints using Sn-58Bi solder only. Whiskers could be directly observed at the fracture surface, and one can clearly see from the enlarged view of zone A that  $\text{Al}_{18}\text{B}_4\text{O}_{33}$  whiskers pinned into and tightly integrated with the solder. However, pull-out whiskers were not observed on the fracture surface

of the copper substrate side. The fracture during solder ball shear testing happened very close to the copper substrate, along the borderline of the solder alloy rather than completely in the composite. Therefore, during the shear test, the whiskers distributed across the fracture were inclined to remain in the removed solder ball. The addition of  $\text{Al}_{18}\text{B}_4\text{O}_{33}$  whiskers improved the shear strength of BGA joints after remelting, and the mechanism can be explained as follows: The solder ball melted and reacted at the surface of the BGA pad when the joint was remelted, and a thin  $\text{Cu}_6\text{Sn}_5$  intermetallic layer was rapidly generated along the interface during the first remelting process.  $\text{Al}_{18}\text{B}_4\text{O}_{33}$  whiskers were inclined to adsorb on the  $\text{Cu}_6\text{Sn}_5$  intermetallic layer due to its high interfacial energy, and some whiskers even adsorbed onto the surface of the copper pad. Therefore, the whiskers around the intermetallic layer could block the Cu/Sn interdiffusion channel. Diffusion was weakened, and thus the growth rate of the  $\text{Cu}_6\text{Sn}_5$  intermetallic layer decreased. Since the  $\text{Cu}_6\text{Sn}_5$  intermetallic layer is more brittle compared with the Sn-Bi solder itself and the shear fracture was gradually inclined to happen in the intermetallic layer, the thinner intermetallic layer could improve the mechanical properties of the BGA joint.

## CONCLUSIONS

Addition of aluminum borate whiskers with diameter of 0.5  $\mu\text{m}$  to 1.5  $\mu\text{m}$  and length of 5  $\mu\text{m}$  to 15  $\mu\text{m}$  dramatically reinforced a tin-bismuth solder due to the high strength and high modulus of the whiskers and a microstructure refinement effect. Coarse brittle Bi-rich phases were restrained by well-embedded whiskers, and the lamellar spacing decreased from 0.84  $\mu\text{m}$  to 7.94  $\mu\text{m}$  to the range of 0.22  $\mu\text{m}$  to 1.80  $\mu\text{m}$ . The intermetallic layer thickness grew more slowly during remelting due to the retardation effect of whiskers blocking the Cu/Sn interdiffusion channel. The joint strength was accordingly improved with the whiskers, after both remelting and long-time aging treatment. The shear strength of the composite solder BGA joints was 24.7 MPa, and only declined by 4.9% after remelting for ten cycles, while the shear strength of the joint without whiskers declined remarkably by 31.5% from 19.4 MPa to 13.3 MPa. With whisker addition, the shear strength was 8.5% higher even after 2 weeks of aging treatment.

## ACKNOWLEDGEMENTS

The authors gratefully acknowledge the financial support from the National Natural Science Foundation of China (NSFC, Grant Nos. 51275135, 51474081, 51475103, and 51321061), and The Funds for Distinguished Young Scientists of Heilongjiang Province. The authors thank Mr. Sigurd R. Pettersen (Department of Structural Engineering, Norwegian University of Science and Technology) and Dr. Chunhui Wu (The Institute of Scientific and Industrial Research, Osaka University) for important advice during manuscript preparation.

## REFERENCES

- M. Abtew and G. Selvaduray, *Mater. Sci. Eng. R* 27, 95 (2000).
- C.M.L. Wu, D.Q. Yu, C.M.T. Law, and L. Wang, *Mater. Sci. Eng. R* 44, 1 (2004).
- B. Zaccariba, *Weld. Int.* 15, 545 (2001).
- J. Shen and Y.C. Chan, *Microelectron. Reliab.* 49, 223 (2009).
- H.Y. Lee and J.G. Duh, *J. Electron. Mater.* 35, 494 (2006).
- X. Lv, T. Lin, J. Wang, J. An, and P. He, *Mater. Trans.* 54, 1228 (2013).
- L. Gao, J. Wang, T. Lin, P. He, and F. Lu, *14th International Conference on Electronic Packaging Technology (ICEPT)*, (2013), p. 193.
- Y. Zhou, N. Zhao, C. Shi, E. Liu, X. Du, and C. He, *Mater. Sci. Eng. A* 598, 114 (2014).
- J. Hu, X.F. Wang, and Z.Z. Zheng, *J. Appl. Phys.* 107, 023513 (2010).
- S.C. Tjong and Y.W. Mai, *Compos. Sci. Technol.* 68, 583 (2008).
- J. Yin, D. Yao, H. Hu, Y. Xia, K. Zuo, and Y.P. Zeng, *Mater. Sci. Eng. A* 607, 287 (2014).
- M. Sobhani, H. Arabi, A. Mirhabibi, R.M.D. Brydson, and T. Nonferr, *Metal. Soc.* 23, 2994 (2013).
- H.Q. Gao, L.D. Wang, and W.D. Fei, *Mater. Sci. Eng. A* 479, 261 (2008).
- T. Lin, M. Yang, P. He, C. Huang, F. Pan, and Y. Huang, *Mater. Des.* 32, 4553 (2011).
- Y.S. Tang, G.Z. Liang, Z.P. Zhang, and J. Han, *J. Appl. Polym. Sci.* 106, 4131 (2007).
- Y.C. Feng, L. Geng, G.H. Fan, and A.B. Li, *Mater. Des.* 30, 3632 (2009).
- G.J. Zhang, J.F. Yang, M. Ando, and T. Ohji, *J. Am. Ceram. Soc.* 87, 299 (2004).
- R.J. McCabe and M.E. Fine, *J. Electron. Mater.* 31, 1276 (2002).
- D. Frear, D. Grivas, and J.W. Morris, *J. Electron. Mater.* 16, 181 (1987).
- J.P. Coughlin, J.J. Williams, and N. Chawla, *J. Mater. Sci.* 44, 700 (2009).
- M. Yang, T. Lin, P. He, and Y. Huang, *Mater. Sci. Eng. A* 528, 3520 (2011).
- M. Murugesan, C. Zandén, X. Luo, L. Ye, V. Jokubavicius, M. Syväjärvi, and J. Liu, *J. Mater. Chem. C* 2, 7184 (2014).
- M.K. Mani, G. Viola, M.J. Reece, J.P. Hall, and S.L. Evans, *Mater. Sci. Eng. A* 592, 19 (2013).
- A.A. El-Daly, G.S. Al-Ganainy, A. Fawzy, and M.J. Younis, *Mater. Des.* 55, 837 (2014).
- X. Wang, Y.C. Liu, C. Wei, H.X. Gao, P. Jiang, and L.M. Yu, *J. Alloys Compd.* 480, 662 (2009).
- V. Tvergaard, *Acta Metall. Mater.* 38, 185 (1990).
- X.N. Zhang, L. Geng, and B. Xu, *Mater. Chem. Phys.* 101, 242 (2007).
- Y. Feng, X. Zhou, Z. Min, and W. Kun, *Scripta Mater.* 53, 361 (2005).
- X. Zhang, L. Xu, S. Du, J. Han, P. Hu, and W. Han, *Mater. Lett.* 62, 1058 (2008).
- K. Suganuma, T. Fujita, N. Suzuki, and K. Niihara, *J. Mater. Sci. Lett.* 9, 633 (1990).
- G. Simon and A.R. Bunsell, *J. Mater. Sci.* 19, 3649 (1984).
- G. Bi, H.W. Wang, Q. Wang, R.J. Wu, and D. Zhang, *J. Mater. Sci. Lett.* 20, 799 (2001).
- L.M. Peng, X.K. Li, H. Li, J.H. Wang, and M. Gong, *Ceram. Int.* 32, 365 (2006).
- B. Cherukuri, R. Srinivasan, S. Tamirisakandala, and D.B. Miracle, *Scripta Mater.* 60, 496 (2009).
- M. Amagai, *Microelectron. Reliab.* 48, 1 (2008).
- B. Liu and H.C. Zeng, *Small* 1, 566 (2005).
- Y. Gu, P. Shen, N.N. Yang, and K.Z. Cao, *J. Alloys Compd.* 586, 80 (2014).
- A. Sharma, S. Bhattacharya, S. Das, and K. Das, *Metall. Mater. Trans. A* 44, 5587 (2013).